Imprint stamps

DOI: 10.1002/smll.200600100

Wafer-Scale Ni Imprint Stamps for Porous Alumina Membranes Based on Interference Lithography**

Woo Lee, Ran Ji, Caroline A. Ross, Ulrich Gösele, and Kornelius Nielsch*

In recent years, nanoporous anodic aluminum oxide (AAO) has been intensively exploited as a template material for the preparation of multifunctional nanostructures, which have applications in various scientific and technological fields.[1] In template-based materials synthesis, it is desirable to use a template with long-range order, so that structurally well-defined materials can be subsequently produced. In a typical anodization process, a self-ordered close-packed array of oxide nanopores forms with domain size (ordering length) on a scale of a few micrometers.[2] To achieve a long-range-ordered pore arrangement over a larger area, Masuda and co-workers first developed a pretexturing process that uses a SiC mold to produce ordered arrays of dimples on the Al substrate by nanoindentation prior to anodization.[3] Shallow indentations on an Al substrate initiate pore nucleation during anodization and lead to a long-range-ordered pore arrangement within the stamped area (e.g., 4×4 mm). This work has sparked considerable interest within the growing community of research groups using porous alumina, which is evident from the several hundred citations of these publications within a few years. However, few groups have been able to fabricate large-area, long-range-ordered alumina membranes due to the high processing costs of the imprint stamps, which can be a few thousand US$ for a cm^2 pattern.

Recently, alternative methods based on focused ion beams (FIB),[4] optical diffraction gratings,[5] and micro-beads[6] were also used to achieve prepatterning of Al substrates, thus avoiding fabrication of the expensive SiC imprint stamp. More recently, Masuda and co-workers demonstrated the fabrication of ideally ordered AAO films with a sub-50-nm pore interval by employing metal molds, which were fabricated by replication from a resist pattern prepared by electron-beam lithography (EBL).[7] While each of these methods have their own advantages, most of them have limitations in scalability. Consequently, the simple and economic realization of long-range-ordered AAO over very large areas (cm^2 to wafer size) still presents challenges.

Herein, we propose two inexpensive approaches for the development of large-scale metallic stamps, which can then be used to imprint Al (see Figure 1). The processes consist of two steps: the replication of Ni imprint stamps from a master pattern, and the subsequent fabrication of long-range-ordered AAO by anodization of Al prepatterned using the Ni stamps. In method I, the imprint stamp is replicated once by electrodeposition onto a large-scale periodic photoresist pattern, similar to the method described in ref. [7]. However, instead of using EBL, the periodic photoresist patterns in the present work were fabricated by laser interference lithography (LIL), which allows the production of periodic nanostructures with a high throughput.[8] Pattern transfer by imprint lithography onto metallic substrates such as Al requires 50 to 2000 times higher pressures in comparison to imprint lithography on polymer layers.[9] Due to the high mechanical stresses, damage to the imprint stamp often occurs after several uses, so it is advantageous to be able to make multiple imprint stamps from a single master. This has motivated the development of an alternative approach

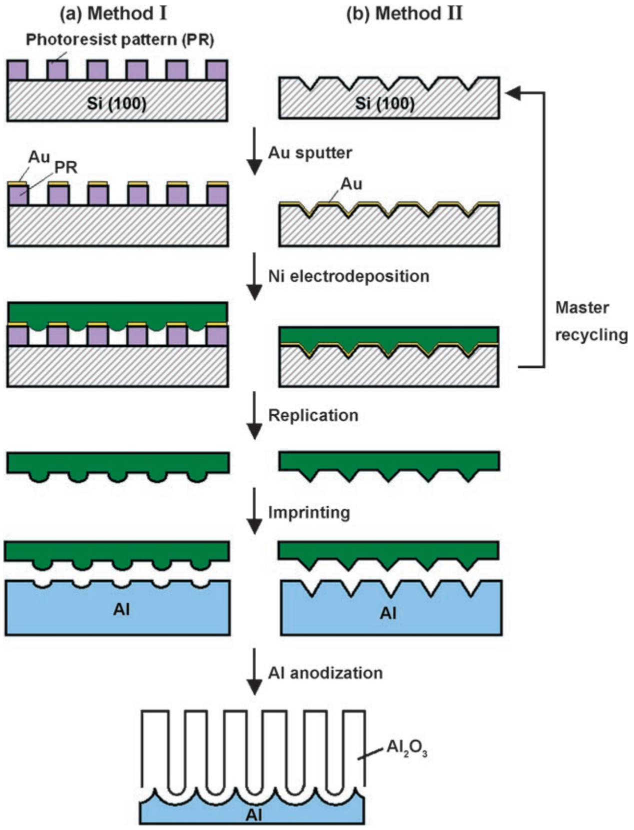

Figure 1. Schematic diagram of the fabrication of ideally ordered anodic alumina using Ni imprint stamps that can be replicated from a) a resist pattern (method I) and b) a silicon pattern (method II).

---

[*] Dr. W. Lee, R. Ji, Prof. Dr. U. Gösele, Dr. K. Nielsch
Max Planck Institute of Microstructure Physics
Weinberg 2, 06120 Halle (Germany)
Fax: (+49) 345-5511223
E-mail: woolee@mpi-halle.de

Prof. Dr. C. A. Ross
Department of Materials Science and Engineering
77 Massachusetts Avenue, Cambridge, MA 02139 (USA)

[**] Financial support from the German Federal Ministry for Education and Research (BMBF, Project No. 03N8701) and the National Science Foundation are greatly acknowledged. We would like to thank Dr. Mato Knez for AFM investigations and Prof. H. I. Smith of MIT for the use of laboratory facilities and valuable discussions.

Supporting information for this article is available on the WWW under http://www.small-journal.com or from the author.

(termed method II), in which a strategy for making the imprint stamp commonly used in soft-imprint lithography is applied.[10] A robust Si master with an array of inverted pyramid etch pits (see Experimental Section) was created by interference lithography, reactive ion etching, and wet-chemical etching. The Si master pattern itself is not employed in the imprint process, but a large number of imprint stamps can be replicated from it.

In method I, after double exposure and development of the resist, the resist patterns were used for the replication of Ni imprint stamps via electrodeposition (see Experimental Section). Figure 2 shows representative SEM images of resist patterns with hexagonal (Figure 2a) and square (Figure 2b) symmetry, together with micrographs of the respective free-standing Ni replicas (Figure 2c and d). LIL produced arrays of uniform-sized holes in the resist over the entire sample area (typically 4 in. in diameter). The periodicity of the pattern was adjusted by controlling the incident angle of exposure, and the symmetry of the lattice by controlling the angle between the two successive LIL exposures (60° for hexagonal, 90° for square symmetry). The holes on the resist patterns with a hexagonal lattice show a slightly elongated shape along the [210] direction of the 2D lattice due to the intensity distribution of the double exposure of the laser interference fringes. The surface of the replicated Ni films consists of an array of bumps with elliptical (in the hexagonal array) or circular (in the square array) shapes and rounded tops, which match the geometry of the holes in the resist.

The replicated Ni films were used as imprint stamps for the prepatterning of electropolished Al substrates. Typically, nanoindentation of the Al was achieved by applying a pressure of about 25 kN cm^{-2} for 10 s using an oil press. The present Ni imprint stamps have a sufficiently high mechanical strength for nanoindentation of Al, and AFM investigations revealed that there was no apparent structural deformation of the surface features of the Ni imprint stamp even after it had been used five times.

After nanoindentation, anodization was conducted under a constant voltage of 156 V in 5 wt% H_3PO_4 at 0.5 °C. Each of the shallow indentations created by imprinting serves as a nucleation site for the development of a pore in the early stages of anodization, and results in the eventual growth of a pore channel. The anodization voltage was chosen to satisfy the linear relationship between interpore distance and anodization potential (2.5 nm V^{-1}).[11] Figure 3 shows representative SEM images of the as-prepared anodic alumina with hexagonal (Figure 3a) and square (Figure 3b) arrangements of pores, together with an oblique view of the cross sections of the respective samples (Figure 3c and d). Straight oxide nanochannels with uniform-sized pores were obtained. However, as the oxide thickness increased, the initial periodic arrangement of the pores eventually became perturbed. Samples with a hexagonal arrangement of pores maintained a well-ordered pore lattice up to a pore aspect ratio (length/inner diameter) typically over 120, but samples with a square lattice of pores maintained long-range order only up to an oxide thickness of about 3 μm, which corresponds to an aspect ratio of 15.

In addition, the geometrical shape of the pore channels was governed by the symmetry of the imprint stamp. The as-prepared AAO with a hexagonal arrangement of holes (Figure 3a) has circular openings at the pore mouth surface. In contrast, the pores of the sample with a square lattice (Figure 3b) have rectangular cross sections. These differences became more apparent when the pores of the as-prepared AAO were enlarged by wet-chemical etching with 5 wt% H_3PO_4 at 45 °C. These observations are in line with the experimental findings of Masuda et al.,[12] in which the initial shape of the openings in an as-prepared AAO changes from circular to square through an etching treatment, due to the slower etching rate of the anion-free inner wall of the cells compared to the anion-incorporated outer wall.[11a,13]

Additionally, this imprint stamp has been successfully used for the growth of long-range-ordered alumina membranes with smaller interpore distances than the stamp periodicity via a templated self-assembly strategy during the anodization process (see Supporting Information).[14]

The photoresist patterns used in method I served as an excellent

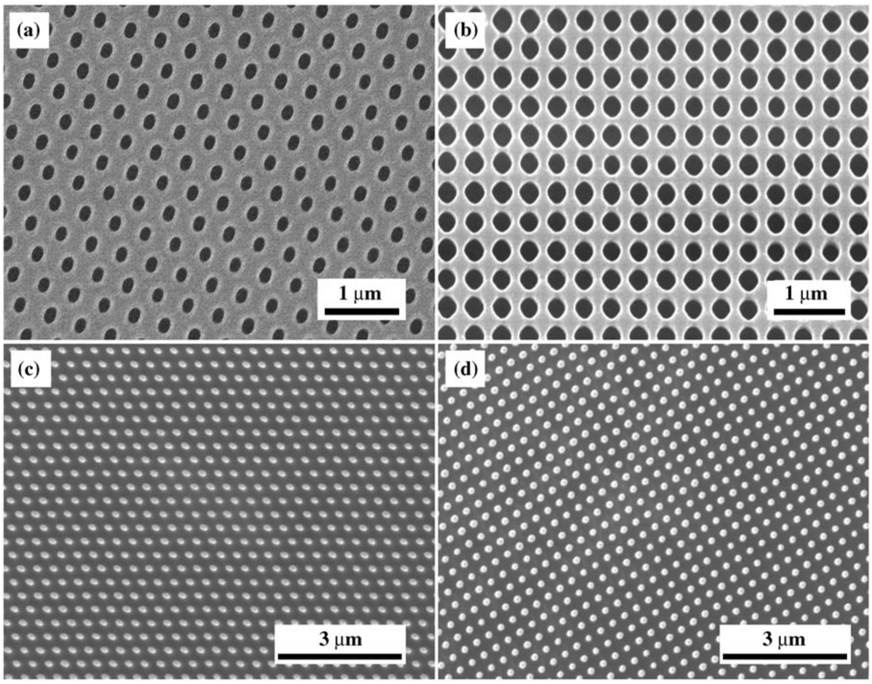

Figure 2. Representative SEM images of resist patterns with a) hexagonal and b) square arrangements of holes, and of Ni imprint stamps with an array of imprint tips in c) hexagonal and d) square lattices.

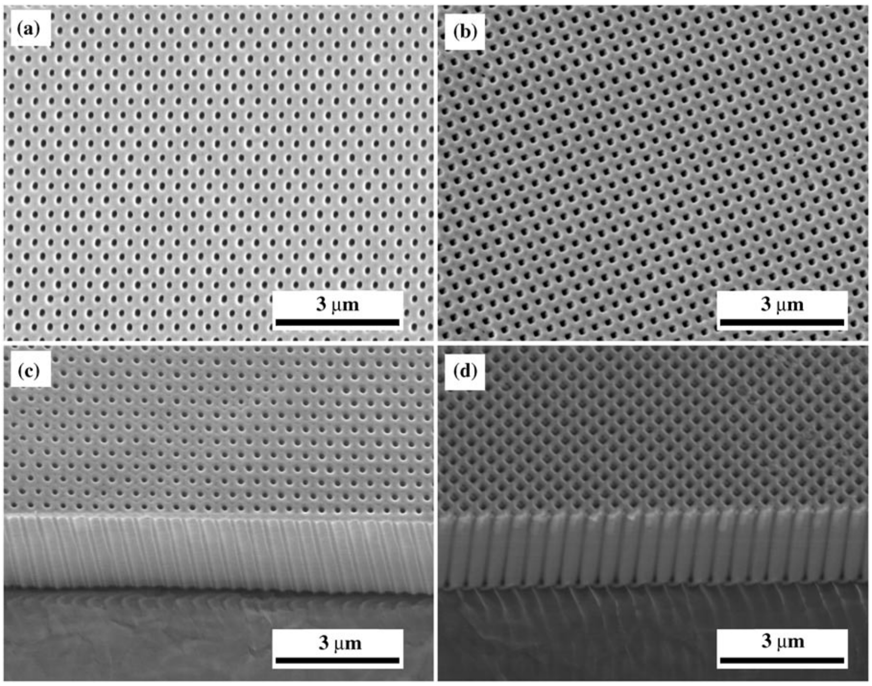

Figure 3. SEM micrographs of long-range-ordered anodic alumina with a) hexagonal and b) square arrangements of nanopores. c, d) Oblique views of the cross sections.

master for the replication of Ni imprint stamps by electrochemical deposition. However, the resist patterns have a disadvantage in terms of reusability for the replication process, due to the poor mechanical durability of the resist and its weak adhesion to the substrate. In method II, a process to fabricate reusable master patterns with good mechanical durability was developed. The lithographic patterning is also based on the LIL technique, but in this case the 2D arrangement of holes in the resist is transferred into the Si(100) substrate using a combination of reactive ion etching (RIE) and anisotropic wet-chemical etching to generate an array of well-defined etch pits with inverted pyramid structures (see Experimental Section).

Figure 4 a shows a typical SEM micrograph of a silicon master with a rectangular arrangement of etch pits with an average interval of 180 nm in one direction and 207 nm in the other direction. The Ni imprint stamps were replicated according to the procedure shown schematically in Figure 1 b. This procedure is similar to that of method I, except for an additional step involving the modification of the surface of the Si master with organosilane molecules just prior to Au sputtering. Surface modification was achieved by treating the Si master with 3-aminopropyltriethoxysilane (3-APTES; 1.0 vol % in CH_3CH_2OH) at 65 °C. The self-assembled organosilane layer facilitates the stripping of the Ni replica from the surface of the Si master after the electrodeposition of Ni by acting as an anti-sticking film.[15] As a result, the Si master could be reused 5 to 25 times to produce further imprint stamps.

Figure 4 b shows a surface view of a Ni imprint stamp replicated from the Si master shown in Figure 4 a. The Ni replica has the complementary topography to that of the master Si pattern, with two different lattice constants of 180 and 207 nm. The sharp Ni pyramids provide a more efficient shape for nanoindentation of an Al substrate compared to the rounded tips of the Ni imprint stamp of method I, and this allows a reduced stamping pressure of 5 to 14 $kN\,cm^{-2}$ to be used, which is about half of the pressure needed for the Ni imprint stamps of method I.

Figure 5 shows representative SEM micrographs of nanoporous AAO prepared from Al substrates which were prepatterned using a sharp-tipped imprint stamp by applying 5 $kN\,cm^{-2}$ (Figure 5 a) and 14 $kN\,cm^{-2}$ (Figure 5 b). Anodizations were conducted at 84 V in 0.05 M $H_2C_2O_4$ (oxalic acid) at 1 °C. It is apparent that the pressure applied during imprinting influences not only the geometrical shape but also the size of the pores of the AAO. Anodization of Al imprinted at a low pressure results in relatively small circular pore openings (Figure 5 a), while high-pressure imprinting results in a rectangular shape.

In comparison with our previous approach using Si_3N_4 imprint stamps with pyramidal tips,[14] both approaches presented herein are inexpensive and require fewer process steps, without the need for wafer bonding and mechanical polishing. Method I does not require RIE and is suitable for high-throughput lithography techniques such as LIL or photolithography. Due to the ability to fabricate multiple copies from a single master, method II is also attractive for costly masters made, for example, by electron or focused ion beam techniques. For our previous Si_3N_4 imprint stamp,[14] a patterned Si_3N_4 film a few micrometers in thickness was bonded to a Si wafer. However, microcracks occurred in the Si_3N_4 layer due to the different mechanical properties of Si and Si_3N_4. In comparison with SiC or Si_3N_4 stamps, the Ni imprint stamps exhibit a lower mechanical hardness but do not form microcracks during use, thus allowing multiple uses.

Here we have demonstrated imprint stamps with sub-200-nm periodicity generated by LIL with a He/Cd laser ($\lambda = 325$ nm), but smaller structures are possible based on recent advances in LIL techniques. Achromatic interference lithography can generate sub-100-nm patterns on a cm^2 scale,[16] immersion interference lithography is currently under development,[17] new lasers with shorter wavelengths and higher coherence length have become commercially available for LIL,[18] and 2D patterns with 50-nm periodicity

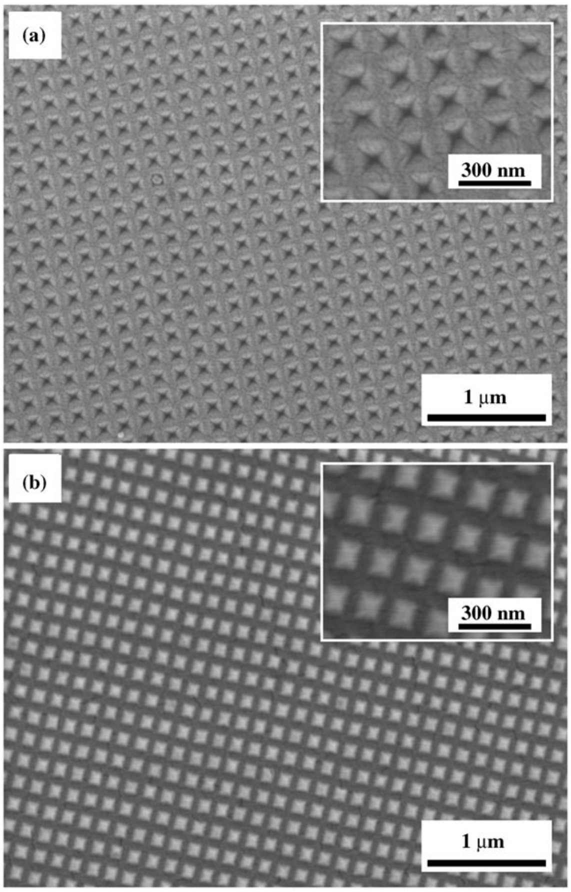

Figure 4. SEM micrographs of a) a silicon master pattern with an array of inverted pyramid etch pits arranged in a square lattice and b) a Ni imprint stamp replicated from the silicon master shown in (a). Magnified SEM images of the respective samples are shown as insets.

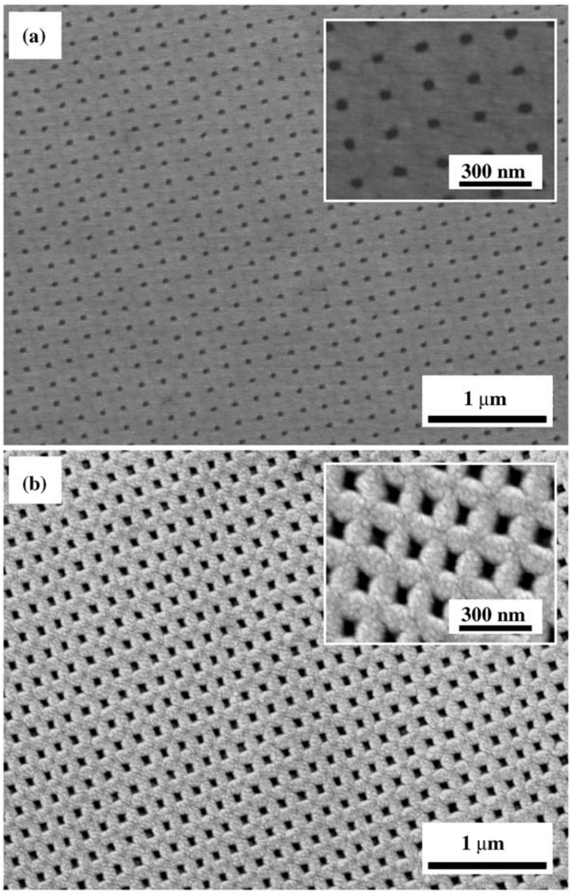

Figure 5. SEM images of anodic alumina films prepared by anodizing Al substrates. The Al surfaces were prepatterned by applying a pressure of a) 5 and b) 14 kN cm^{-2} using a Ni imprint stamp replicated from an etched Si master. Magnified views of the respective samples are shown as insets.

have been made by using synchrotron radiation.[19] We expect that our two approaches for making large-area imprint stamps can be scaled toward smaller structures by using these advanced LIL approaches.

In summary, the fabrication of wafer-scale, long-range-ordered, nanoporous anodic aluminum oxide has been demonstrated by using large-area Ni imprint stamps with arrays of imprint tips in a hexagonal or square lattice. An electrodeposition technique was employed to replicate Ni imprint stamps from substrates that were patterned by laser interference lithography. The Ni imprint stamps could be successfully used up to ten times for the surface prepatterning of Al with a high fidelity in pattern transfer. Anodization of nanoindented Al substrates produced long-range-ordered arrays of oxide pores in hexagonal, square, and rectangular lattices. It is expected that the resulting nanoporous alumina membranes could be used as templates for developing advanced functional nanostructures over areas as large as a whole wafer.

Experimental Section

Preparation of photoresist patterns: For method I, a bilayer stack of a negative-type resist (OHKA TSMR-iN027) with a thickness of 180 nm and an antireflection coating (Wide–8B) with a thickness of 70 nm was used. Exposure dose profiles of laser light were recorded on the resist using a LIL system with a Lloyd's mirror interferometer and a He/Cd laser ($\lambda = 325$ nm) as light source. The periodicity of the pattern could be adjusted from 180 nm up to 2 μm by controlling the incident angle of the laser. Hexagonal or square patterns were made by double exposure and rotation of the sample by 60° or 90° between the two exposures, respectively. The exposed resist was developed using Ohka NMD-W 2.38%.

Preparation of silicon master patterns: For method II, a trilayer stack of a negative resist (Ohka THMR-*i*N PS-4) 200 nm in thickness, a sputter-deposited SiO_2 interlayer 20 nm in thickness, and an antireflection coating (BARLî) 185 nm in thickness was deposited on a Si(100) wafer coated with 40 nm of thermal oxide. After exposure and development of the resist, the pattern was transferred through the SiO_2 interlayer, the antireflection coating, and the layer of thermal SiO_2 by four RIE steps with

CHF_3, O_2, CHF_3, and O_2 gases, respectively. The final RIE step with O_2 stripped the remaining resist. The patterned Si(100) wafer was then anisotropically etched using a short HF dip followed by immersion in a KOH solution. The surface of the resulting Si master was derivatized with organosilane molecules. To optimize the silanization procedures, the surface of the Si was cleaned to remove any contamination and thereafter activated to increase the density of reacting OH groups. The Si surface was cleaned by immersing the sample in Piranha solution (H_2SO_4/H_2O_2; 3:1) for 30 min with intermediate ultrasonication. Surface modification was achieved by treating the resulting Si with 3-aminopropyltriethoxysilane (3-APTES; 1.0 vol% in CH_3CH_2OH) at 65 °C.

Electrodeposition of Ni: A thin Au film was plasma-sputtered onto the resist pattern using a conventional sputter coater for SEM to make the surface of the polymer pattern electrically conductive. This Au layer served as a working electrode in the subsequent electrodeposition of the metal. Ni was electrodeposited on the resist pattern using a Ni plating solution comprising $NiCl_2 \cdot 6H_2O$ (8.41×10^{-2} M), $Ni(H_2NSO_3)_2 \cdot 4H_2O$ (1.59 M), and H_3BO_3 (0.33 M). The typical current density was 7 mA cm^{-2}. The thickness of the nickel film could be conveniently controlled by changing the amount of total integrated charge involved in the electrochemical reaction. After the electrodeposition, Ni imprint stamps with a thickness of ≈5 µm were obtained by stripping the metal film from the resist pattern.

Keywords:
alumina · anodization · electrodeposition · lithography · templates

---

[1] a) N. I. Kovtyukhova, T. E. Mallouk, *Adv. Mater.* **2005**, *17*, 187–192; b) K.-B. Lee, S. Park, C. A. Mirkin, *Angew. Chem.* **2004**, *116*, 3110–3112; *Angew. Chem. Int. Ed.* **2004**, *43*, 3048–3050; c) S. J. Son, J. Reichel, B. He, M. Schuchmann, S. B. Lee, *J. Am. Chem. Soc.* **2005**, *127*, 7316–7317; d) W. Lee, M. Alexe, K. Nielsch, U. Gösele, *Chem. Mater.* **2005**, *17*, 3325–3327; e) F. Matsumoto, K. Nishio, H. Masuda, *Adv. Mater.* **2004**, *16*, 2105–2108; f) Z. Liang, A. S. Susha, A. Yu, F. Caruso, *Adv. Mater.* **2003**, *15*, 1849–1853; g) W. Lee, R. Scholz, K. Nielsch, U. Gösele, *Angew. Chem.* **2005**, *117*, 6204–6208; *Angew. Chem. Int. Ed.* **2005**, *44*, 6050–6054; h) T. Yanagishita, Y. Tomabechi, K. Nishio, H. Masuda, *Langmuir* **2004**, *20*, 554–555; i) S. B. Lee, D. T. Mitchell, L. Trofin, T. K. Nevanen, H. Soderlund, C. R. Martin, *Science* **2002**, *296*, 2198–2200.

[2] a) A. P. Li, F. Müller, A. Birner, K. Nielsch, U. Gösele, *J. Appl. Phys.* **1998**, *84*, 6023–6026; b) H. Masuda, K. Yada, A. Osaka, *Jpn. J. Appl. Phys.* **1998**, *37*, L1340–L1342.

[3] a) H. Masuda, H. Yamada, M. Satoh, H. Asoh, M. Nakao, T. Tamamura, *Appl. Phys. Lett.* **1997**, *71*, 2770–2772; b) H. Asoh, K. Nishio, M. Nakao, T. Tamamura, H. Masuda, *J. Electrochem. Soc.* **2001**, *148*, B152–B156.

[4] C. Y. Liu, A. Datta, Y. L. Wang, *Appl. Phys. Lett.* **2001**, *78*, 120–122.

[5] I. Mikulskas, S. Juodkazis, R. Tomasiumas, J. G. Dumas, *Adv. Mater.* **2001**, *13*, 1574–1577.

[6] a) S. Fournier-Bidoz, V. Kitaev, D. Routkevitch, I. Manners, G. A. Ozin, *Adv. Mater.* **2004**, *16*, 2193–2196; b) H. Masuda, Y. Matsui, M. Yotsuya, F. Matsumoto, K. Nishio, *Chem. Lett.* **2004**, *33*, 584–585.

[7] K. Yasui, K. Nishio, H. Nunokawa, H. Masuda, *J. Vac. Sci. Technol. B* **2005**, *23*, L9–L12.

[8] a) C. A. Ross, H. I. Smith, T. Savas, M. Schattenburg, M. Farhoud, M. Hwang, M. Walsh, M. C. Abraham, R. J. Ram, *J. Vac. Sci. Technol. B* **1999**, *17*, 3168–3176; b) M. Farhoud, J. Ferrera, A. J. Lochtefeld, T. E. Murphy, M. L. Schattenburg, J. Carter, C. A. Ross, H. I. Smith, *J. Vac. Sci. Technol. B* **1999**, *17*, 3182–3185.

[9] S. Y. Chou, P. R. Krauss, P. J. Renstrom, *Appl. Phys. Lett.* **1995**, *67*, 3114–3116.

[10] Y. Xia, G. M. Whitesides, *Angew. Chem.* **1998**, *110*, 568–594; *Angew. Chem. Int. Ed.* **1998**, *37*, 550–575.

[11] a) S. Ono, N. Masuko, *Corros. Sci.* **1992**, *33*, 503–507; b) S. Ono, N. Masuko, *Surf. Coat. Technol.* **2003**, *169*, 139–142.

[12] H. Masuda, H. Asoh, M. Watanabe, K. Nishio, M. Nakao, T. Tamamura, *Adv. Mater.* **2001**, *13*, 189–192.

[13] a) G. E. Thompson, G. C. Wood, *Nature* **1981**, *290*, 230–232; b) P. P. Mardilovich, A. N. Govyadinov, N. I. Mazurenko, R. Paterson, *J. Membr. Sci.* **1995**, *98*, 143–156.

[14] J. Choi, K. Nielsch, M. Reiche, R. B. Wehrspohn, U. Gösele, *J. Vac. Sci. Technol. B* **2003**, *21*, 763–766.

[15] a) M. Beck, M. Graczyk, I. Maximov, E.-L. Sarwe, T. G. I. Ling, M. Keil, L. Montelius, *Microelectron. Eng.* **2002**, *61–62*, 441–448; b) M. Keil, M. Beck, T. G. I. Ling, M. Graczyk, L. Montelius, B. Heidari, *J. Vac. Sci. Technol. B* **2005**, *23*, 575–584; c) Y. Xu, W. Zhao, H. Y. Low, *Microelectron. Eng.* **2006**, *83*, 542–546.

[16] T. A. Savas, M. L. Schattenburg, J. M. Carter, H. I. Smith, *J. Vac. Sci. Technol. B* **1996**, *14*, 4167–4170.

[17] W. C. Cheng, L. A. Wang, *J. Vac. Sci. Technol. B* **2003**, *21*, 3078–3081.

[18] Deep-UV (DUV) solid-state lasers, Sony Precision Technology Inc., Cobalt UW-1020A, frequency-quadrupled Nd:YAG 266 nm, coherence length >100 m.

[19] L. J. Heyderman, H. H. Solak, C. David, D. Atkinson, R. P. Cowburn, F. Nolting, *Appl. Phys. Lett.* **2004**, *85*, 4989–4991.

Received: February 28, 2006